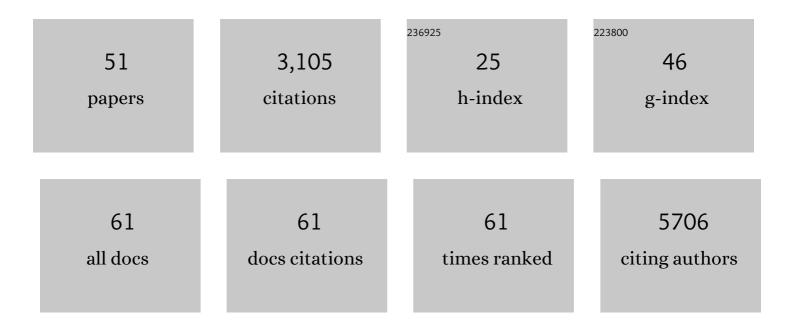
## **Thomas Boudier**

List of Publications by Year in descending order

Source: https://exaly.com/author-pdf/2465709/publications.pdf Version: 2024-02-01



THOMAS ROUDIER

#	Article	IF	CITATIONS
1	TANGO: a generic tool for high-throughput 3D image analysis for studying nuclear organization. Bioinformatics, 2013, 29, 1840-1841.	4.1	648
2	Three-Dimensional Architecture of Presynaptic Terminal Cytomatrix. Journal of Neuroscience, 2007, 27, 6868-6877.	3.6	280
3	TomoJ: tomography software for three-dimensional reconstruction in transmission electron microscopy. BMC Bioinformatics, 2007, 8, 288.	2.6	264
4	Electron tomography of early melanosomes: Implications for melanogenesis and the generation of fibrillar amyloid sheets. Proceedings of the National Academy of Sciences of the United States of America, 2008, 105, 19726-19731.	7.1	133
5	DiAna, an ImageJ tool for object-based 3D co-localization and distance analysis. Methods, 2017, 115, 55-64.	3.8	132
6	Analysis of synaptic ultrastructure without fixative using high-pressure freezing and tomography. European Journal of Neuroscience, 2006, 24, 3463-3474.	2.6	128
7	Tangentially Migrating Neurons Assemble a Primary Cilium that Promotes Their Reorientation to the Cortical Plate. Neuron, 2012, 76, 1108-1122.	8.1	127
8	A-type Lamins Form Distinct Filamentous Networks with Differential Nuclear Pore Complex Associations. Current Biology, 2016, 26, 2651-2658.	3.9	127
9	Macrophages provide a transient muscle stem cell niche via NAMPT secretion. Nature, 2021, 591, 281-287.	27.8	111
10	Progerin reduces LAP2α-telomere association in Hutchinson-Gilford progeria. ELife, 2015, 4, .	6.0	96
11	Structural basis for delta cell paracrine regulation in pancreatic islets. Nature Communications, 2019, 10, 3700.	12.8	80
12	Multiple binding of repressed mRNAs by the P-body protein Rck/p54. Rna, 2012, 18, 1702-1715.	3.5	79
13	From high-resolution AFM topographs to atomic models of supramolecular assemblies. Journal of Structural Biology, 2007, 159, 268-276.	2.8	70
14	Effector and stem-like memory cell fates are imprinted in distinct lymph node niches directed by CXCR3 ligands. Nature Immunology, 2021, 22, 434-448.	14.5	66
15	3D FISH for the quantification of methane- and sulphur-oxidizing endosymbionts in bacteriocytes of the hydrothermal vent mussel <i>Bathymodiolus azoricus</i> . ISME Journal, 2008, 2, 284-292.	9.8	61
16	Structural Information, Resolution, and Noise in High-Resolution Atomic Force Microscopy Topographs. Biophysical Journal, 2009, 96, 3822-3831.	0.5	51
17	Biomineralization Patterns of Intracellular Carbonatogenesis in Cyanobacteria: Molecular Hypotheses. Minerals (Basel, Switzerland), 2016, 6, 10.	2.0	48
18	Smart 3D-fish: Automation of distance analysis in nuclei of interphase cells by image processing. Cytometry Part A: the Journal of the International Society for Analytical Cytology, 2005, 67A, 18-26.	1.5	41

THOMAS BOUDIER

#	Article	IF	CITATIONS
19	Software for drift compensation, particle tracking and particle analysis of highâ€speed atomic force microscopy image series. Journal of Molecular Recognition, 2012, 25, 292-298.	2.1	39
20	A generic classification-based method for segmentation of nuclei in 3D images of early embryos. BMC Bioinformatics, 2014, 15, 9.	2.6	36
21	Shifting meiotic to mitotic spindle assembly in oocytes disrupts chromosome alignment. EMBO Reports, 2018, 19, 368-381.	4.5	30
22	A new automated 3D detection of synaptic contacts reveals the formation of cortico-striatal synapses upon cocaine treatment in vivo. Brain Structure and Function, 2015, 220, 2953-2966.	2.3	29
23	An Erg-driven transcriptional program controls B cell lymphopoiesis. Nature Communications, 2020, 11, 3013.	12.8	29
24	Organising multi-dimensional biological image information: The BioImage Database. Nucleic Acids Research, 1999, 27, 280-283.	14.5	28
25	High-Speed Atomic Force Microscopy: Cooperative Adhesion and Dynamic Equilibrium of Junctional Microdomain Membrane Proteins. Journal of Molecular Biology, 2012, 423, 249-256.	4.2	27
26	Rapid Synaptogenesis in the Nucleus Accumbens Is Induced by a Single Cocaine Administration and Stabilized by Mitogen-Activated Protein Kinase Interacting Kinase-1 Activity. Biological Psychiatry, 2017, 82, 806-818.	1.3	27
27	Electron tomography of biological samples. Biochemistry (Moscow), 2004, 69, 1219-1225.	1.5	25
28	Functional Assessment of Genetic Variants with Outcomes Adapted to Clinical Decision-Making. PLoS Genetics, 2016, 12, e1006096.	3.5	24
29	Multiple-axis tomography: applications to basal bodies from Paramecium tetraurelia. Biology of the Cell, 2006, 98, 415-425.	2.0	23
30	The site of breast cancer metastases dictates their clonal composition and reversible transcriptomic profile. Science Advances, 2021, 7, .	10.3	23
31	Video on the Internet: An Introduction to the Digital Encoding, Compression, and Transmission of Moving Image Data. Journal of Structural Biology, 1999, 125, 133-155.	2.8	22
32	Simultaneous localization of MLL, AF4 and ENL genes in interphase nuclei by 3D-FISH: MLL translocation revisited. BMC Cancer, 2006, 6, 20.	2.6	18
33	A novel toolbox to investigate tissue spatial organization applied to the study of the islets of Langerhans. Scientific Reports, 2017, 7, 44261.	3.3	17
34	EM-stellar: benchmarking deep learning for electron microscopy image segmentation. Bioinformatics, 2021, 37, 97-106.	4.1	16
35	Use of cryo-negative staining in tomographic reconstruction of biological objects: application to T4 bacteriophage. Biology of the Cell, 2003, 95, 393-398.	2.0	14
36	OpenSegSPIM: a user-friendly segmentation tool for SPIM data. Bioinformatics, 2016, 32, 2075-2077.	4.1	14

THOMAS BOUDIER

#	Article	lF	CITATIONS
37	Analysis of Nuclear Organization with TANGO, Software for High-Throughput Quantitative Analysis of 3D Fluorescence Microscopy Images. Methods in Molecular Biology, 2015, 1228, 203-222.	0.9	14
38	Persistent homology for object segmentation in multidimensional grayscale images. Pattern Recognition Letters, 2018, 112, 277-284.	4.2	13
39	Proliferation-dependent positioning of individual centromeres in the interphase nucleus of human lymphoblastoid cell lines. Molecular Biology of the Cell, 2015, 26, 2550-2560.	2.1	12
40	A novel generic dictionary-based denoising method for improving noisy and densely packed nuclei segmentation in 3D time-lapse fluorescence microscopy images. Scientific Reports, 2019, 9, 5654.	3.3	12
41	Direct Image-Based Correlative Microscopy Technique for Coupling Identification and Structural Investigation of Bacterial Symbionts Associated with Metazoans. Applied and Environmental Microbiology, 2011, 77, 4172-4179.	3.1	11
42	Tomography of bacteria–mineral associations within the deep-sea hydrothermal vent shrimp Rimicaris exoculata. Comptes Rendus Chimie, 2008, 11, 268-280.	0.5	10
43	EM-net: Deep learning for electron microscopy image segmentation. , 2021, , .		9
44	Chromosomes distribute randomly to, but not within, human neutrophil nuclear lobes. IScience, 2021, 24, 102161.	4.1	8
45	NucleiNet: A convolutional encoder-decoder network for bio-image denoising. , 2017, 2017, 1986-1989.		7
46	VIDOS, a system for video editing and format conversion over the Internet. Computer Networks, 2000, 34, 931-944.	5.1	4
47	Optimal processing for gel electrophoresis images: Applying Monte Carlo Tree Search in GelApp. Electrophoresis, 2016, 37, 2208-2216.	2.4	3
48	A dictionary-based approach to reduce noise in fluorescent microscopy images. , 2017, , .		2
49	Detection of high-grade atypia nuclei in breast cancer imaging. , 2015, , .		1
50	3D Analysis and Reconstruction of the Chitin Secreting Gland of Riftia pachyptila. Journal of Biological Systems, 1997, 05, 445-456.	1.4	0
51	TAPAS: Towards Automated Processing and Analysis of multi-dimensional bioimage data. F1000Research, 2020, 9, 1278.	1.6	Ο